Development Status of an Open Capillary Pulsed Plasma Thruster with Non-Volatile Liquid Propellant

IEPC-2013-291

Presented at the 33rd International Electric Propulsion Conference,
The George Washington University, Washington, D.C., USA
October 6–10, 2013

S. Barral[1], J. Kurzyna[2]
Institute of Plasma Physics and Laser Microfusion, 01497 Warsaw, Poland

E. Remírez[3], R. Martín[4]
JMP Ingenieros, 26371 Sotés (la Rioja), Spain

P. Ortiz[5], J. Alonso[6]
Najera Aerospace, 26371 Sotés (la Rioja), Spain

S. Bottinelli[7], Y. Mabillard[8]
Mecartex, 6933 Muzzano, Switzerland

A. Zaldívar[9], P. Rangsten[10]
NanoSpace AB, Uppsala Science Park, SE-751 83 Uppsala, Sweden

and

C. R. Koppel[11]
KopooS Consulting Ind., 75008 Paris, France

A novel type of Pulsed Plasma Thruster (PPT) based on an open capillary design and on a non-volatile liquid propellant is currently under development within the Liquid Micro Pulsed Plasma Thruster FP7 project (L-µPPT). Its design is expected to improve over PTFE-based PPTs by providing significant increase in total impulse, increased propellant utilization, lower impulse bit variability and the possibility to balance propellant requirements between several thrusters with a common tank. The current development status of the project is reported, covering the key design choice and current level of testing of the first thruster prototype, its power processing and control unit, propellant tank, dedicated thrust balance, propellant micropump and vacuum facility. An analysis of several mission scenarios is also reported which highlights the potential of the system.

[1]Research associate, Division of Magnetized Plasmas, serge.barral@ipplm.pl.
[2]Research associate, Division of Magnetized Plasmas, jacek.kurzyna@ipplm.pl.
[3]Chief executive officer, eduardo.remirez@jmpingenieros.es.
[4]Project manager, ricardo.martin@jmpingenieros.es.
[5]Electronic system design engineer, pablo.ortiz@nasp.es.
[6]Electronic system design engineer, javier.alonso@nasp.es.
[7]Chief executive officer, stefano.bottinelli@mecartex.ch.
[8]Head of R&D, yann.mabillard@mecartex.ch.
[9]Development engineer,Ana.Salaverri@sscspace.com.
[10]Vice president engineering, pelle.rangsten@sscspace.com.
[11]Chief consulting engineer, christophe.koppel@kopoos.com.

Nomenclature

c_p	specific heat capacity
E	discharge energy
F	thrust
g_0	standard gravitational acceleration, $g_0 \equiv 9.80665\,\mathrm{m\,s^{-2}}$
I_{bit}	impulse bit
I_{sp}	specific impulse
I_{ssp}	system specific impulse
I_t	total impulse
m_α	molecular mass of species α
$\dot{M}$	propellant mass flow rate
M_{prop}	total propulsion system mass
M_{dry}	dry propellant mass
$M_{S/C}$	total spacecraft mass
N	total number of discharges during thruster lifetime
ΔV	velocity increment
η	thruster efficiency
κ	Boltzmann constant, $\kappa \equiv 1.3806488 \times 10^{-23}\,\mathrm{m^2 kg\,s^{-2} K^{-1}}$
λ	thermal conductivity
ρ	propellant mass density

I. Introduction

The desire to reduce development and launcher costs and the narrow focus of many payloads has in recent years driven the development of very small platforms in the kg range. Such spacecrafts have benefited from the wider availability of enabling technologies (micro/nano-fabrication), but remain hindered by the lack of sufficiently compact and lightweight micro-propulsion systems. Low thrust propulsion systems have at the same time also become a critical component in a number of scientific missions that require fine positioning, such as space-based telescope interferometers, imaging arrays and formation flying missions.[1] Due to their simplicity and scalability, Pulsed Plasma Thrusters (PPT) are increasingly considered for small delta-V missions on nano-spacecrafts.[2,3]

The goal of the L-µPPT project is the development and assessment of a novel PPT technology based on an open capillary design and on a non-volatile liquid propellant, which in comparison to conventional solid-propellant (PTFE) PPTs is expected to offer significantly larger total impulse and lower impulse bit variability throughout the thruster lifetime. Another intrinsic advantage of liquid propellant is the possibility to balance propellant requirements between several thrusters with a common tank, which in practice is expected to enable to a twofold increase in propellant utilization.

The liquid propellant PPT concept was pioneered by Ziemer at Princeton's EEPDyL in the late 1990's. Water was then investigated as a prospective replacement for argon in a gas-fed PPTs,[4] and was injected in a vapor (gaseous) state through a fast gas valve. Because the response time of gas valves largely exceeds than the transit-time of the gas between the electrodes, Ziemer proposed to generate a train of several tens of discharge pulses with a repetition period lower that the transit time so as to warrant that all propellant introduced during one valve cycle is utilized. This strategy proved successful, but the mass penalty associated with the requirement of multiple capacitor banks makes it unpractical for space applications.

Later experiments by other researchers have attempted to forego the use of a gas valve, as in the water PPT experiment led by Scharlemann at Ohio State University where the liquid-to-gas phase transition was operated within a porous injector.[5] Although it was theorized by the authors that gas feeding would be suspended between subsequent discharges, to the best of our knowledge this hypothesis has not been substantiated by experimental measurements. In the most documented research to date on liquid propellant PPTs performed at the University of Tokyo by Kakami and Koizumi between 2003 and 2005,[6,7,8,9] water was in turn fed in liquid state by a custom drop-on-demand electromechanical injector. Ongoing research

efforts on water PPTs in China[10] and in Germany[11] have not yet attempted to resolve the issue of propellant injection and use continuous water vapor injection.

It is notable that all past and current liquid propellant PPT projects have focused on water propellant, due in particular to its chemical inertness and reduced spacecraft contamination as redeposition of solid products is avoided. From an application viewpoint, however, two significant drawbacks of water are its relatively high freezing point and its volumetric expansion upon freezing, which pose important challenges on nanosatellites where active thermal management is usually not an option. From a thruster design perspective, in turn, the high volatility makes efficient implementations of water-propelled PPTs extremely intricate, as discussed in section A.

The many issues associated with the use of water as propellant and current lack of compelling solution to address them has motivated the L-µPPT project to adopt a non-volatile liquid that can be easily used and stored over a wide temperature range. These properties have been leveraged to implement a tighter control of the propellant mass bit than in PTFE-based PPTs, which is expected to lead to improvements in terms of impulse bit predictability and propellant utilization efficiency (*i.e.* the relative amount of injected propellant that actually gets accelerated).

Following the outline of the main motivations and conceptual design of the L-µPPT system in section II, an overview of the current status of the propulsion sub-systems including thruster, electronics, propellant tank, propellant delivery sub-system are provided in section III, followed by a description of the testing facility and thrust balance in section IV. Finally, a short mission analysis study is reported in section V that highlight the prospective advantages and possible applications of the system under development.

II. Conceptual design

A. Critical assessment of water-propellant PPTs

A key problem in the design of water-propellant PPTs is the high vapor pressure of water. Because it rapidly evaporates in open space, valve-less designs such as those used in several of the above-mentioned liquid propellant PPTs[5,10,11] are not likely to reach practical viability: assuming a pulse repetition frequency of 1 Hz and a typical discharge duration of 10 μs, only 0.001% of the propellant would be actually used, the remaining 99.999% being wasted between subsequent discharges. It is therefore not entirely surprising that no efficiency measurement has ever been published in respect of valve-less PPTs. Our critical review will thus focus on Princeton's gas valve design and on Tokyo's drop-on-demand valve design, which are the only existing concepts where the propellant utilization issue was considered.

It is useful at first to assess the characteristic residence time of a water molecule in the discharge gap. Assuming a characteristic device dimension of the order of $\ell = 1$ cm and a temperature $T = 300$ K, the residence time can be estimated as:

$$t_r \approx \ell \sqrt{\frac{m_{H_2O}}{\kappa T}} \approx 27\,\mu\text{s} \tag{1}$$

which is only a few time larger than the typical duration of a PPT discharge. Because even fast gas valves cannot offer actuation times comparable with the residence time of relation (1), an original solution was developed at Princeton to ensure high propellant utilization whereby pulse trains of some 30-100 discharge per valve opening were triggered. By using a high repetition rate within each pulse train, propellant waste was significantly reduced and very high efficiencies (for PPTs) of the order of 20% were reportedly achieved. This multi-burst concept appears thus very effective in resolving the propellant utilization issue, but presents significant drawbacks: increased complexity, reduced reliability (gas valve cycling, discharge misfires) and very large capacitor bank. For nanosatellites, the mass penalty incurred by the required 30-100 fold increase of the capacitor bank size irremediably disqualifies this solution.

The approach taken at the University of Tokyo could more easily lends itself to miniaturization, but doubts remain regarding its real-life performances. A drop-on-demand (DOD) injection system was developed to inject single water droplets in the channel. Although the efficiencies initially reported were high, up to 13%,[6,7] the efficiency of a latter design did not exceed 6% despite it being presented by its authors as an improvement over the former thruster.[9] From a theoretical perspective, even a 6% efficiency appears difficult to explain, since, as the authors have themselves demonstrated theoretically,[9] only about 20% of the water in a droplet ejected in vacuum is vaporized before the droplet freezes. Since this vaporization occurs over time scales of the order of 1 ms ($20 - 50$ times greater than the discharge duration), propellant

utilization and efficiency would in principle be limited to 1%. The reasons for the high efficiency reported remains unknown but it is possible that the efficiency has been overestimated as a result of ablated electrode material acceleration, which in small PPTs is known to even enable "propellant-less" propulsion.[12]

B. Key design choices

1. *Propellant*

The critical review of injection systems performed in section A exposes a number of issues that put into question the practical feasibility of water propellant PPTs, especially for nano-spacecrafts where sub-zero temperatures can be met and where the mass of a multi-burst capacitor bank is unacceptable. For this reason, the retained solution fundamentally departs from prior liquid PPT designs and relies instead on a low vapor pressure liquid propellant.

The main low vapor pressure prospective propellants that have been considered are high vacuum lubricants such as mineral oils, silicone oils and perfluoropolyether (PFPE) fluids. Although ionic liquids are currently under consideration for colloid ion thrusters, they were discarded due to their relatively low chemical stability and very high freezing point. Their high electrical conductivity is, besides, incompatible with the spark ablation solution adopted in the L-μPPT design. Among high vacuum lubricants, PFPE fluids clearly stand out due to the following properties:

- exceptionally low evaporation rate in vacuum up to $100 - 150$ °C,
- non-hazardous,
- excellent chemical stability,
- liquid phase stable over a very wide temperature range,
- routinely in use and space-qualified for spacecraft mechanical components lubrication,
- fluoropolymer composition, *i.e.* very close to that of PTFE (Teflon), which is already qualified as space propellant due to its wide use on conventional PPTs,
- good dielectric properties compatible with the flashover spark ablation method adopted in the L-μPPT,
- high storage density.

Its only intrinsic disadvantage compared to water is the potential redeposition of carbon, although it is from this perspective no worse than the PTFE propellant used in conventional PPTs. Its chemical and thermal stability also makes it much more attractive than the EMI-BF_4 ionic liquid commonly used in colloid ion thrusters.

2. *Ablation method*

In order to avoid propellant waste before and/or after the discharge it is critical that the injector vaporizes or ablates the required amount of propellant within a period shorter than the residence time of gas molecules in the discharge volume.

The vaporization of droplets by conductive heat transfer, for instance with a micro-heater,[9] does not appear sufficiently fast for this purpose. Indeed, the characteristic conductive heat transfer time for a layer of thickness h can be deduced from the propellant's thermal diffusivity by,

$$t_{cond} \approx \frac{\rho c_p}{\lambda} h^2 \tag{2}$$

where we can take the approximate values $\lambda = 0.1\ \mathrm{W\,m^{-1}K^{-1}}$, $\rho = 1500\ \mathrm{kg\,m^{-3}}$ and $c_p = 1000\ \mathrm{J\,kg^{-1}K^{-1}}$. Taking h of the order of the radius of a droplet ($h \approx 0.1\,\mathrm{mm}$), this gives $t_{cond} \approx 0.15$ s, which is about 10^4 times larger than the gas molecules residence time within the discharge domain.

An ablative process appears thus required to warrant sufficiently rapid phase change. Laser ablation by means of a diode laser is in principle an option, but this method is difficult to implement owing to the very low light absorption of the chosen propellant at the wavelengths of currently available high power pulsed laser diodes. Although less repeatable, flashover surface ablation with an electrical discharge is a much simpler and lightweight option. This method relies on a high voltage spark gap above the propellant's surface, which is not only meant to ignite the main discharge — as in the case of conventional PPT spark gaps — but also to ablate the propellant to be accelerated by the main discharge.

Liquid propellant PPTs have thus the unique capability to achieve a separation of the ablation and acceleration processes. Indeed, by feeding the propellant in a small capillary it is possible to permanently

keep the free surface of the propellant in the close vicinity of the spark gap and thus to significantly enhance the ablation generated by the spark gap. On the other hand, since the cross-section of the capillary is about 100 times smaller than the exposed propellant surface in a Teflon PPT of similar size (1 mm^2 vs 1 cm^2), ablation by the main discharge is expected to be negligible and the so-called late time ablation held responsible for the low efficiency of solid-propellant PPTs can hopefully be avoided.

In order to assess the order of magnitude of the required spark gap discharge energy, it is necessary to estimate the energy required to heat up and vaporize the nominal propellant mass bit. Based on general data for this type of fluid, the vaporization heat is assumed less than $\Delta H_v \approx 50\ \mathrm{kJ \cdot kg^{-1}}$. Since the specific heat of the propellant is close to $1000\ \mathrm{J \cdot kg^{-1} K^{-1}}$, the energy necessary to heat up the propellant from room temperature to its decomposition temperature ($\approx 250°\mathrm{C}$) is less than $250\ \mathrm{kJ \cdot kg^{-1}}$. Therefore, the energy necessary to heat up and vaporize a mass bit of $M_{bit} = 5\ \mu\mathrm{g}$ of propellant is of the order of 1.5 mJ only. Obviously the energy coupling between the spark gap and the propellant surface is rather poor, despite the fact that the capillary is located just near the spark gap. Even if one assumes only a 5% energy coupling, however, the energy of the spark gap would not exceed 30 mJ, which represents only a small fraction of the main discharge energy.

3. General thruster operation

The conceptual design of the L-μPPT is shown on Fig. 1. The propellant flow rate is controlled by a volumetric dispensing device such as a micropump. A spark gap discharges is regularly triggered near the capillary end, which rapidly vaporizes and partially ionizes a small amount of propellant. The generated ionized vapor triggers in turn the main discharge which accelerates the propellant via Lorentz forces, as in a conventional PPT.

The L-µPPT operation exploits the fact that the energy coupling between the spark gap and the propellant to be vaporized decreases when the free surface of the liquid recedes inside the capillary. This causes the free surface to adjust its position in the capillary in such a way that the ablated volume remain equal to the volume dispensed by the pump between subsequent discharges. Provided that the propellant mass flow rate delivered by the pump is constant, the injection/ablation process is thus a closed-loop process able to accommodate for cyclic and long term changes such as propellant temperature, spark gap wear, etc, in such a way that the ablated volume always remains nearly equal to the volume dispensed between discharges. The stabilization of this self-regulated process can be accelerated by increasing the non-linearity of the relationship between energy coupling and free surface position, *e.g.* by changes in the capilary and ablation electrode geometry.

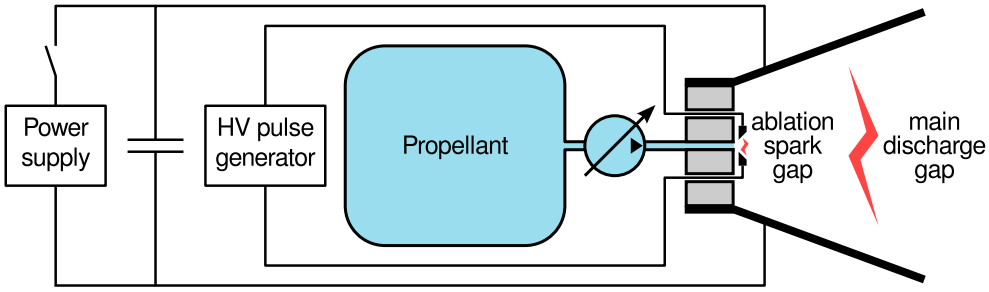

Figure 1. Conceptual design of the L-μPPT showing propellant delivery by a micro-pump into an open capillary, propellant ablation by a spark gap and its subsequent acceleration by a conventional PPT discharge.

III. Thruster development status

The L-µPPT implementation follows a 2-phase development path where 2 prototypes —a proof-of-concept and a breadboard demonstrator— are to be designed and tested in succession for each of the thruster subsystems and for the thrust balance. The below development status exclusively relates to the proof-of-concept development phase.

A. Thruster body with integrated miniature syringe pump

1. *Main parameters*

The target parameters were primarily determined from the power and mass budget of typical CubeSats and from a mission analysis summarized in section V. A maximum footprint of 1/3 U CubeSat, that is 333 g and 333 cm^3, has been adopted as the long term target for a single thruster system, which is meant to include the thruster, the capacitors, the tank, the propellant and the electronics. Although this requirement was relaxed for the proof-of-concept prototype, the thruster remains relatively light at around 80 g including capacitors and miniature syringe pump but excluding interfacing parts and electronics[a]. Due to the possibility to store propellant in a tank, the targeted total impulse is at least 100 N s per thruster, which is well beyond the state of the art for similarly sized solid propellant PPTs.

A nominal shot energy of $E = 2$ J at 1500 V is targeted, which should enable operation at a maximum frequency of 1 Hz in a small CubeSat. Accounting for voltage-dependent capacitance de-rating, the target energy was achieved with 20 ceramic capacitors arranged in a 10×2 parallel-series configuration.

Unlike solid propellant PPTs where the propellant mass is intrinsically limited by the geometry (*e.g.* 10 g for Mars Space Ltd's thruster which also targets CubeSats[13]), the propellant in the L-µPPT is mainly constrained by the total system mass and volume. A nominal propellant mass of $M_{prop} = 85$ g was selected, which should provide a total impulse in excess of 500 N s.

It must be underlined, however, that the total mass imposes stringent requirements on the capacitors. Indeed, the number of pulses to fully utilize the propellant can be calculated as:

$$N = \frac{1}{2}\frac{g_0 I_{sp} I_t}{\eta E} = \frac{1}{2} M_{prop} \frac{g_0^2 I_{sp}^2}{\eta E}.$$

Based on typical data from the literature reported in table 1, we shall take $I_{sp} = 600$ s and $\eta = 4\%$ to infer that the expected number of discharge pulses would be around 18 10^6, which is very significant for high voltage pulse capacitors. This relationship also underlines the counter-intuitive negative impact of high I_{sp} on capacitor lifetime. As discussed in section V, the I_{sp} is fortunately nearly irrelevant in small propulsion systems since propellant mass is typically much less than the dry system mass, meaning that the high I_{sp} of water PPTs actually makes them less attractive than solid propellant PTFE thrusters due to requirement in terms of capacitor lifetime. This provides another rationale for the chosen propellant, which owing to its similar molecular composition is expected to provide an I_{sp} in the same range as PTFE thrusters. Because a probable flight configuration would employ 4 thrusters fed by a common 85 g tank, the lifetime requirement would actually drop below 5×10^6 pulses per capacitor bank. Given the criticality of capacitor lifetime, however, capacitor testing has been undertaken early on in the project using custom test benches. As of today, the targeted 5×10^6 pulses capacitor lifetime has been demonstrated for capacitors with slightly lower capacitance and slightly higher nominal voltage than used in the first prototype. Capacitor testing is ongoing to determine the lifetime *vs* voltage relationship and to improve the soldering procedure.

Based on the typical ratio of mass bit to discharge energy in table 1, the nominal mass bit was set to 5 μg. Note, however, that this nominal mass bit was merely used as a ballpark figure for the design of the miniature pump, since the mass bit can be in principle freely set by the energy of the spark ablation electrodes.

2. *Syringe pump*

The aforementioned nominal mass bit of 5 μg corresponds to a volume of approximately 3 nl of propellant. For technological reasons, however, it is desirable to relax the dosing volume requirement so as to enable larger pump strokes which could be dispensed only every few discharges.

[a] note that no tank is used in the proof-of-concept thruster prototype, although a tank prototype has been developed to be tested separately, see section C

	Propellant	E [J]	I_{sp} [s]	I_{bit} [μN · s]	m_{bit}/E [μg · W^{-1}]	η [%]
Mars Space Ltd[2]	PTFE	1.7	590	28	2.8	4.7
LES-6[14]	PTFE	1.85	300	26	4.8	2
MPACS[15]*	PTFE	1.96	827	80	5.0	16
Dawgstar[16]	PTFE	5.23	483	56.1	2.3	2.6
AFRL MicroPPT[17,18]*	PTFE	6.6	-	10	-	-
SMS[14]	PTFE	8.4	450	133	3.5	3.7
LP-PPT[7,9]†	H_2O	13.5	3400	85	0.2	11

Table 1. Performances of various µPPTs and low power PPTs. (*) Data marked with a star is subject to caution due to very limited and/or inconsistent published information. (†) The LP-PPT has demonstrated impulse bits largely independent from the mass bit and from the propellant, which points to a possible electrode-erosion "propellant-less" operation;[12] the fact high efficiencies were achieved only when the mass bit was the smallest appear to further confirm this hypothesis.

The maximum dosing requirement assumes that the quantity of ablated propellant depends mainly on the distance between the free surface of the propellant inside the capillary and the spark gap. Since both the spark gap and the capillary have characteristic dimensions of the order of the millimeter, it seems reasonable to assume that energy coupling between the spark gap and the fluid will not be strongly affected if the position between the free surface inside the capillary and the electrodes varies by $\delta \approx 0.1$ mm. Assuming a capillary diameter $d_c = 1$ mm, the maximum dosing volume that would fulfill the tolerance set forth is therefore:

$$\delta \frac{\pi d_c^2}{4} \approx 80 \text{ nl} \tag{3}$$

which is more than an order of magnitude larger than the volume to be ablated.

Most micro-pumps commercially available today are piezo-actuated diaphragm pumps built with various elastomer and polymer materials,[19,20,21] which are in general poorly suited to operation in vacuum, have relatively large stroke volumes (several tens of μl) and are optimized for high mass flow rate rather than dosing accuracy. Although their development is more recent, silicon diaphragm pumps appear much more attractive in our application due to their intrinsic vacuum compatibility and very small size. For this reason, the development of a MEMS pump was undertaken by NanoSpace. In order to mitigate risks and meet the tight development schedule of the proof-of-concept thruster prototype, it was decided, however, that the initial thruster would integrate a custom miniature syringe pump as MEMS manufacturing imposes a relatively long development cycle. For this reason, the propellant tank (see section C) and injector (see section 1) are not integrated with the first thruster prototype and are tested separately.

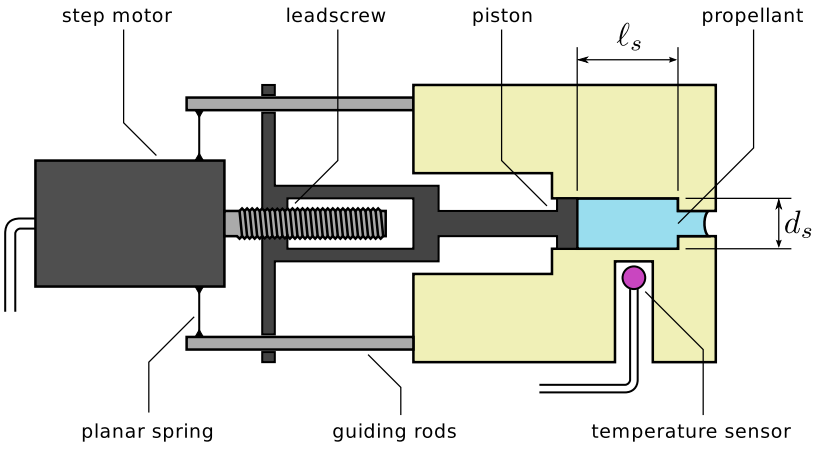

Figure 2. Schematic layout of the syringe pump.

The syringe pump is schematically shown in Fig. 2. The syringe diameter and length are respectively

$d_s = 2\,\text{mm}$ and $\ell_s = 8\,\text{mm}$, which corresponds to a full syringe volume slightly greater than $25\,\mu\text{l}$. This is the equivalent of 3 hours and 20 minutes of continuous operation at 1 Hz with a 3 nl volume bit ($m_{bit} \approx 5\,\mu\text{g}$) per discharge. The syringe volume was chosen as a trade-off between syringe capacity and impact of propellant thermal expansion on the injected volume. Indeed, the volumetric thermal expansion of the propellant is of the order of $\alpha_v \approx 10^{-3}\,\text{K}^{-1}$, meaning that a spurious flow rate of some $0.4\,\text{nl}\,\text{s}^{-1}$ would be observed with a full syringe if the temperature of the thruster were to increase by 1 K every minute. Therefore, active control is required to adjust the volume of the syringe as a function of the propellant temperature during thruster warm-up. In order to warrant an accurate and meaningful assessment of the propellant temperature, a miniature precision NTC thermistor is placed near the syringe and the temperature gradients within the syringe itself are minimized by the use of a very high thermal conductivity ceramic housing. Using priorly measured thermal expansion data, the onboard microcontroller moves the piston back-and-forth to compensate for propellant volume variations.

The step motor is an AM1020 PreciSTEP motor with a resolution of 20 steps per rotation, which can reportedly operate in ultra high vacuum.[22] Accounting for the 0.2 mm leadscrew pitch, the volume stroke is 31 nl per step which easily satisfies requirement 3.

3. Current development status

The complete thruster assembly, shown in Fig. 3, has been manufactured and integrated with the electronics. The operation of the syringe pump with active thermal control has been successfully tested in air and in vacuum (10^{-5} mbar). Propellant ablation tests are currently ongoing in air and shall be shortly performed in vacuum prior to general testing of the complete discharge process.

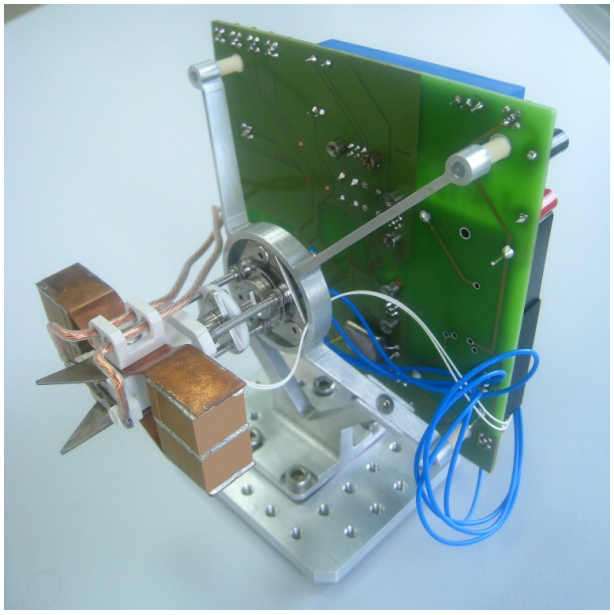

Figure 3. General view of the thruster, showing the main (triangular) electrodes, the small ablation electrodes, the syringe pump and the power processing and control unit mounted on the back of the thruster.

B. Electronics

An integrated power processing and control unit (PPCU) has been manufactured which fits on a $100 \times 100\,\text{mm}^2$ PCB.

The PPCU has a number of functions, among which:

- DC-DC conversion from 12 V to the various voltages required by low-power electronics,
- DC-DC conversion from 12 V to up to 3 kV for the charge of the main capacitor bank,
- $10 - 20$ kV pulse generation for the ablation spark gap using an ignition transformer,
- step motor control,
- thruster temperature measurement,

- capacitor bank voltage measurement during charging phase,
- active control of the syringe pump,
- general management of the charge/discharge, spark ablation and propellant feed sequence,
- serial communication with the monitoring system.

Most control functions and measurement are managed by the on-board Cortex-M3 based microcontroller. Fast voltage and current measurements during the capacitor bank discharge are performed externally by means of voltage probes and Rogowski coils.

C. Propellant tank

With an overall dimension of $100 \times 100 \times 24\,\mathrm{mm}^3$ and a dry mass of 276 g, the first tank prototype easily fits within the targeted 1/3 U CubeSat footprint (1/3 of the volume and mass of a 1U CubeSat). The tank holds $50\,\mathrm{cm}^3$ of propellant, and the assembly is designed to enable its integration with other subsystems (propellant dispensing, thruster and electronics).

One of the goals of tank was to feed the propellant to the dispensing subsystem while avoiding trapped bubbles that could potentially affect thruster operation. A dual-body syringe design was chosen to avoid any transient pressure loss and propellant starvation at the tank outlet. The tank is a monolithic dual-syringe body with top and bottom crosspieces; it accommodates pistons, covers, springs, o-rings, screws, bleed screws, fittings and a pressure sensor. The materials used are Al7075 T6, AISI 304 steel and Viton©, all of which are widely used in space systems.

Figure 4. First prototype of the propellant tank.

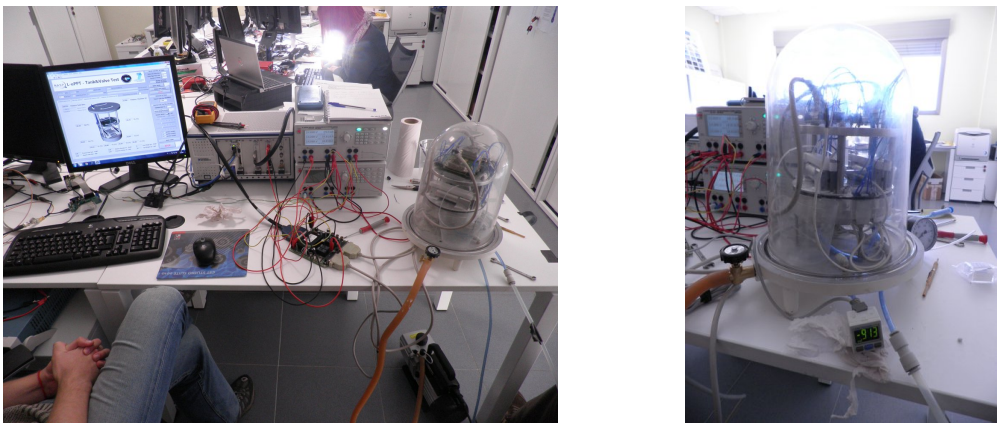

Figure 5. Preliminary propellant tank testing.

The maximum tank pressure of approximately 0.65 bar (relative) is reached when the tank is completely full and the precision springs are fully compressed. Pistons are equipped with double o-ring seals to prevent

any risk of leakage. A test bench was designed and manufactured to test the behavior of the tank and delivery subsystem in vacuum (down to 10^{-6} mbar) at different temperatures. Four Peltiers elements, one in every corner of the tank, are used to cool and heat the entire tank (-20 to +60°C) in a controlled manner. The Peltier's cold junction is kept at a uniform temperature with a water-cooled heat exchanger. A total of eigth NTC thermistors (4 located on the tank surface and 4 on the Peltier´s cold junction) are used to assess the tank's temperature and to monitor the heat exchanger's temperature.

The outlet of the tank is connected to a miniature valve, described farther in section 1.

D. Propellant Dispensing

1. *Injector*

It was initially anticipated that the injector would inject microdroplets into the main electrode gap at each discharge, which vaporization would trigger the main discharge. The injector was expected to work in a DOD mode, a method proposed earlier by Koizumi *et al.*[6,7] However, based on a critical review of existing liquid-propellant PPTs (section A), a spark gap ablation method was ultimately preferred and a change of propellant feeding method from DOD to volumetric delivery was proposed. From a design point of view this meant that, instead of supplying a very small, well defined droplet at each discharge, the injector was required to feed a controlled volume to the ablation capillary.

For the proof-of-concept development, a conventional miniature solenoid valve was selected to dispense minute volumes of the selected propellant from the spring-loaded dual-body propellant tank (section C). Since the chosen valve is not rated for such high viscosities and low pressures, microfluidic testing on component level was performed. Theoretical minimum dispensing volumes (opening time) down to a single micro-liter was confirmed and the valve's operation was characterized at various pressures and temperatures.

2. *Microfluidic experiments*

Micro Electro Mechanical System (MEMS) is the prime candidate technology when a high degree of integration and miniaturization is needed. With its heritage from micro electronic manufacturing processes very, very small components and complex system can be built. Using this technology almost all kinds of different components can be manufactured and achieve complexity and intelligence packed in a very dense volume.

In parallel to the valve dispensing tests preparatory work for the final prototype has been performed. First, capillary feeding in MEMS-fabricated channels and nozzles was performed. The objective was to evaluate the propellant feeding in small capillaries etched in silicon. Figure 6 shows how the propellant is capillary-fed to form a 1 mm meniscus.

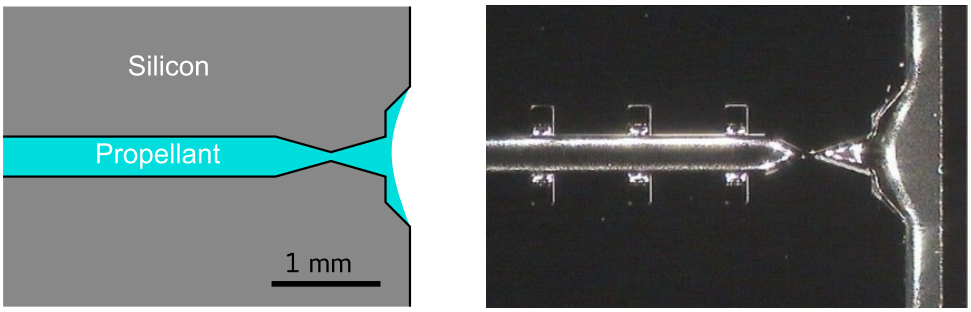

(a) (b)

Figure 6. (a) Drawing of the propellant (blue) capillary fed in the silicon (grey) channel forming a 1 mm meniscus of propellant. (b) Photo of the propellant filled silicon chip.

Secondly, the revised requirements for the final prototype also made it necessary to supply a volumetric rate of a few nanoliter/second with a volumetric accuracy of 5%, and a maximum dispensed volume of around 50 nl, *i.e.* much less than the first microliter-range feeding. This motivates a micropump-based feeding system, which in turn prompted the development of MEMS valves to be used in a micropump configuration in the final prototype of the L-µPPT thruster.

During the proof-of-concept phase, MEMS valves were fabricated and initial development tests performed. The development testing has so far only been qualitative, but has proven that the MEMS valves are functional

with liquid (water). The valves are fabricated from four fusion bonded silicon wafers. Each valve chip includes four individual paraffin actuated valves. The flow can be regulated proportionally to the stroke of the valves by adjusting the power applied to internal paraffin heaters. A set of three valves connected in series enable the implementation of a volumetric pump based on the peristaltic principle, illustrated by Fig. 7.

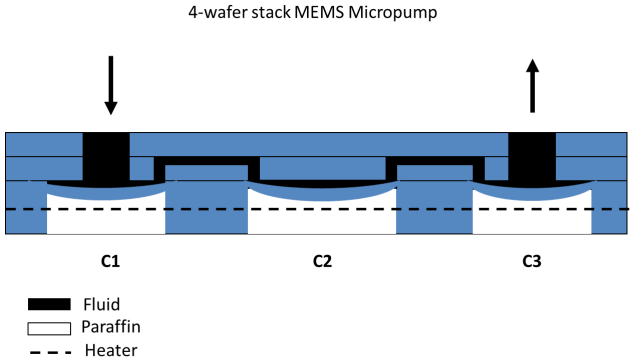

Figure 7. Cross-section of a schematic MEMS pump design based on three paraffin actuators. Paraffin is white and the propellant is visualized in black.

IV. Test facility and thrust stand

A. Vacuum chamber and pumping

The PLANS electric propulsion laboratory was specifically set up at IPPLM to host the L-µPPT test facility, shown in Fig. 8. The vacuum chamber's volume is approximately $2.2\,\mathrm{m}^3$ for a $\varnothing 1.2\,\mathrm{m}$ diameter. An oil-free vacuum pumping system provides an ultimate pressure at the level of 2×10^{-7} mbar for an empty chamber. The turbomolecular pump has a pumping speed of $3000\,\mathrm{l\,s}^{-1}$ (N_2) and is backed by a multistage roots pump of maximum speed $450\,\mathrm{m}^3\mathrm{h}^{-1}$. The pumping enables continuous propellant pumping during thruster operation while maintaining the pressure under 10^{-5} mbar.

The spark ablation process is very sensitive, however, to gases and liquids absorbed in the vicinity of the spark gap as these may provide a path of least resistance during the initial stage of flashover discharges. In order to warrant space-like conditions where the flashover discharge is expected to occur over an almost pure surface of propellant with a fully outgassed thruster, it is important to prevent the condensation of molecular layers between successive discharges. A ten-fold improvements in pumping capacity is expected with a cryogenic pump upgrade, however, which shall provide vacuum levels closer to actual space conditions in low earth orbit and prevent any significant build-up of re-condensed products, thus increasing the repeatability of discharge pulses.

B. Thrust balance

Both the construction and the design of the thrust balance significantly depart from that of former impulse bit measurement balances from the literature.[23,24,25,8,26,27,28]

Because it does away with the rotating arm design used in most impulse bit balances, the L–µPPT balance is very compact (see Fig. 8). Its construction relies on precision machined flexures which impart a very high stiffness in the two directions perpendicular to the thrust, whereas in the direction of the thrust the stiffness can be adjusted over a very wide range. Linear actuators are used to level the base plate and ensure that the rest position of the pendulum is close to the zero of the position sensor. A non-contact actuator is used to calibrate the thrust balance. Frequent calibration is not mandated, however, since the frequency of the pendulum motion subsequent to a pulse provides real-time information about the stiffness during the measurement which is used to compensate for thermal or other environmental drifts. The amplitude of the pendulum motion and the knowledge of the balance's stiffness provides in turn the impulse bit.

Although tests with the thruster have not yet been performed, artificial impulse bits have been generated after the thrust balance was installed in the vacuum chamber which have confirmed the ability of the balance to accurately measure impulse bits of some tens of $\mu\mathrm{N\,s}$.

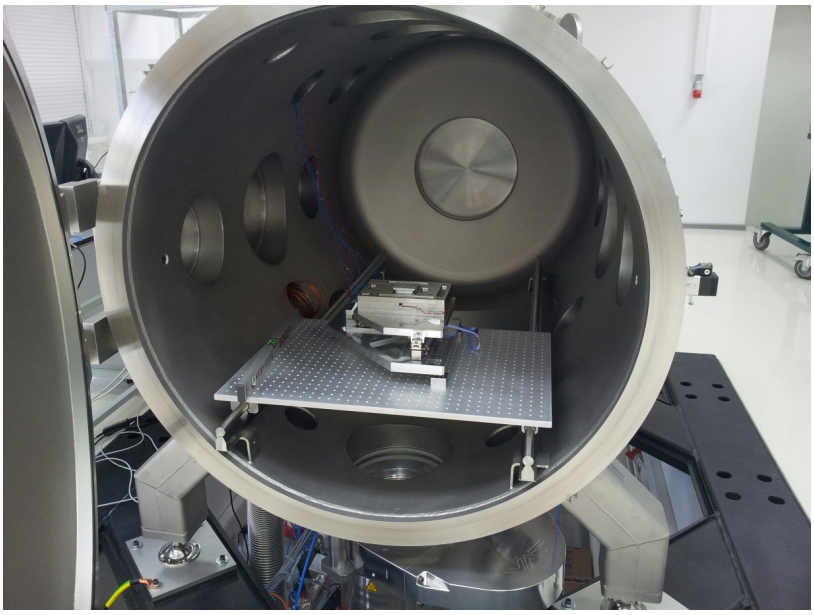

Figure 8. Front view of the vacuum chamber with the thrust stand mounted on a sliding optical breadboard.

V. Mission analysis

A. Performance index of propulsion sub-systems

The most important performance index for spacecrafts is, in general, the *specific impulse*. I_{sp} is defined through the ratio of the total impulse by the mass of propellant used to provide such total impulse, and can be written in several equivalent forms:

$$I_{sp} = \frac{F}{g_0 \dot{M}}, \tag{4}$$

$$= \frac{\int F\, dt}{g_0 M_{prop}}, \tag{5}$$

$$= \frac{I_t}{g_0 M_{prop}}, \tag{6}$$

where I_t is the total impulse generated by the usable propellant mass onboard. However, the I_{sp} does not play any significant role for Picosat or CubeSats size when the dry mass of the propulsion sub-system is of the same order (or sometimes up to 100 times larger) than the propellant mass. The concept of *system specific impulse*, I_{ssp}, introduced by Erichsen[29] can be seen as very relevant to state on the sustainability of one concept of propulsion sub-systems against the others because it include the system mass and the propellant mass. The I_{ssp} is defined as the ratio of the total impulse by the total mass of the propulsion system (dry mass) and its propellant, where the dry mass may include the electrical power system if propulsion is the main user:

$$I_{ssp} = \frac{I_t}{g_0 \left(M_{prop} + M_{dry}\right)}.$$

Table 2 provides a list of demonstrated or expected propulsion sub-systems performance from the literature. Published data show that the thrusters specific impulse, which range from 50 s to 600 s, is always significantly larger than the system specific impulse, which itself varies between 0.6 s and 26 s. For Picosat/Nanosat users, the latter is unfortunately the most relevant figure. It is notable that the largest I_{ssp} (26 s) is achieved by thrusters having an $I_{sp}$of only 100 s, while other propulsion systems which show much higher thrusters specific impulse are in fact characterized by lower system specific impulse. For solid propellant PPTs, moreover, the impossibility to distribute propellant between thrusters can have a sizable impact on the actual propellant

utilization. This highlights the importance of system-level design for propulsion. In order to state on the sustainability of one propulsion concept over another in the context of CubeSat-size spacecrafts, the I_{ssp} must thus be considered the most relevant performance index and the initial goal should therefore be to increase the I_{ssp} to the level of 80 s or higher. For illustration, an I_{ssp} at the level of 160 s would enable a ΔV of 125 $\mathrm{m\,s^{-1}}$ on 3U CubeSats, which would constitute a breakthrough for CubeSats' operations in orbit.

Table 2. System performances for propulsion sub-systems.

	CanX-2	**CanX-2**	**T³µPS**	**MiPS**	**MEPSI**	**µPPT**	**µPPT**
Mission	NANOPS	NANOPS	Delfi-n3Xt	-	MEPSI		
Type	Cold gas	Cold gas	Cold gas	Cold gas	Cold gas	PPT	PPT
Propellant	SF_6	SF_6	solid N_2	C_4H_{10}	Xe	PTFE	PTFE
Manufacturer				Vacco	The Aerospace Corporation	Mars Space Ltd	Mars Space Ltd
Ref.	[30]	[30]	[31]	[32]	[33]	[2]	[13]
M_{dry} [kg]	0.5	0.5	0.12	0.456	0.25	0.15	0.18
M_{prop} [kg]	0.02	0.18	0.0025	0.053	0.05	0.01	0
F [N]	0.05	0.05 ÷ 0.1	0.006 ÷ 0.1	0.055			
I_{bit} [µN s]							34
ΔV [$\mathrm{m\,s^{-1}}$]	2	35		34	20		
$M_{S/C}$ [kg]	4	5		1	1.33		
I_t [N s]	8	175	0.735	34	26.6	29.3	44.0
I_{sp} [s]	50	100	30	65	50	298.5	600.0
I_{ssp} [s]	1.6	26	0.6	6.8	9	19	25

B. Mission profile

At the date of this writing, references to no less that 110 CubeSats can be found in the literature. A review of their needs in terms of propulsion capabilities has been performed which has highlighted the following CubeSat mission sequence:

1. injection on initial deployment orbit (perigee altitude, eccentricity, inclination),
2. achievement of nominal orbit targeted for operation (in general, circular orbit altitude, inclination), including possible large ΔV requirement for interplanetary missions,
3. in-orbit operation, attitude pointing constrains (in general earth pointing), orbit and formation flying maintenance,
4. de-orbit phase.

Recent literature also points to an emerging trend for propulsion applications, namely Attitude Control Systems (ACS) where propulsion is competitive with other methods in terms of mass, power and cost budget. Indeed, owing to the tiny dimensions of CubeSats, reaction wheels (RW) are difficult to build without static or dynamic imbalance. Although propulsion is not a fundamental requirement for attitude control, with a sufficiently large I_{sp} the propellant mass budget required to unload RWs could be less than the 90 g footprint of a 3-axis magneto-torquer systems. This mass budget and the savings in terms of volume would constitute an advantage if the propulsion system is mandated by the mission for other reasons (although this imposes a minimum of 4 thrusters).

A full replacement of RWs by an electric propulsion (EP) subsystem has been considered in a preliminary analysis, where all control is performed by thrusters only[b]. In the case of CubeSats, this translates into a requirement for the propulsion system in terms of number of pulses. Table 3 shows a comparison between classic ACS and active "All EP" ACS with PPTs. The classic ACS considered relies on RWs and is based on published data[35] for a micro-RW. It highlights the specific advantages of the active "All EP" ACS with PPT.

[b] see *e.g.* Ref. 34 for an attitude and orbit control system exclusively based on EP.

In addition, a simulation of active "All EP" 3-axis attitude control of a CubSat with a simplified logic has been performed using the EcosimPro tool and ESA's propulsion library.[36] The main sources of attitude perturbations are magnetic disturbance torque, drag disturbance torque and Sun pressure disturbance torque. The model used comprises several components, including 4 thrusters, 2 tanks, 4 solar arrays, 6 drag areas and a magnetotorquer (used to produce the magnetic disturbance torque). The logic to automatically commute 2 of the 4 thrusters has been added to the model with a statistical tool in order to provide the first assessments of the ACS. The thrust vectors of all four thrusters are as sketched in Fig. .

The main result for the ACS after 3 and half orbits (20000 s) shows that roll pitch and yaw axis are well controlled within $\pm 0.2°$ after the initial phase to reach the desired attitude. Note that this angular deadband is not an intrinsic limit but rather a result of this particular case study. The zoom on the phase diagram shows that the perturbation torques are well taken into account with a standard parabolic trajectory in the phase diagram, before automatic control activates the thrusters. For roll control (around the x axis), the perturbation torques experienced by the S/C along its orbit change sign and the thrusters are activated when the roll approaches the $+0.2°$ or $-0.2°$ limit. Pitch control (around the y axis) is realized in much the same way, while for yaw control (around the z axis), the thrusters are mainly activated near the $+0.2°$ limit. The outcome of such of simulation allows to set the main specifications for the thrusters to be able to perform an active "All EP" attitude control.

Table 3. Comparison of continuous ACS with reaction wheel and active ACS with PPT.

	RW-1 Reaction wheel Type A / Type B	**PPT**	**Best performer**
Angular Momentum [μN m s]	580 / 100	Not limited	*PPT* RW requires at least 1 desaturation per day
Nom. rotation speed [rpm]	8000	N/A	
Max. rotation speed [rpm]	16000	N/A	
Resolution	0.25 rpm (1LSB in rotation speed)	3–10 µN s (min. impulse bit)	*difficult to assess* RW affected by noise & micro-vibrations
Speed deviation (rms) [rpm]	5 / 8.5	N/A	*PPT*
Nominal Torque [μN m]	23 / 4	3.2	*PPT* $\approx$ *TypeB*
Torque deviation (rms) [μN m]	2.2 / 0.8	none	*PPT*
Micro vibration	yes	no	*PPT*
Power consumption	0.62 W (continuous) (@ nominal speed)	1 J (per pulse)	*PPT*
Standby consumption [W]	0.40	0	*PPT*
Desaturation	3 magneto-torquers or active propulsion	none	*PPT*
Mass [kg] (incl. auxiliary systems)	$0.15 + 0.09 = 0.24$	0.333 (incl. orbit control)	*PPT*
Dimensions	0.2 U	0.3 U (incl. orbit control)	*PPT*
Order of magnitude of cost based on similar systems data: CubeSatShop.com	MAI-100 / 200: 27540 € / 34985 € ISIS MagneTorQuer: 7500.00 €	*TBC*	*TBC*

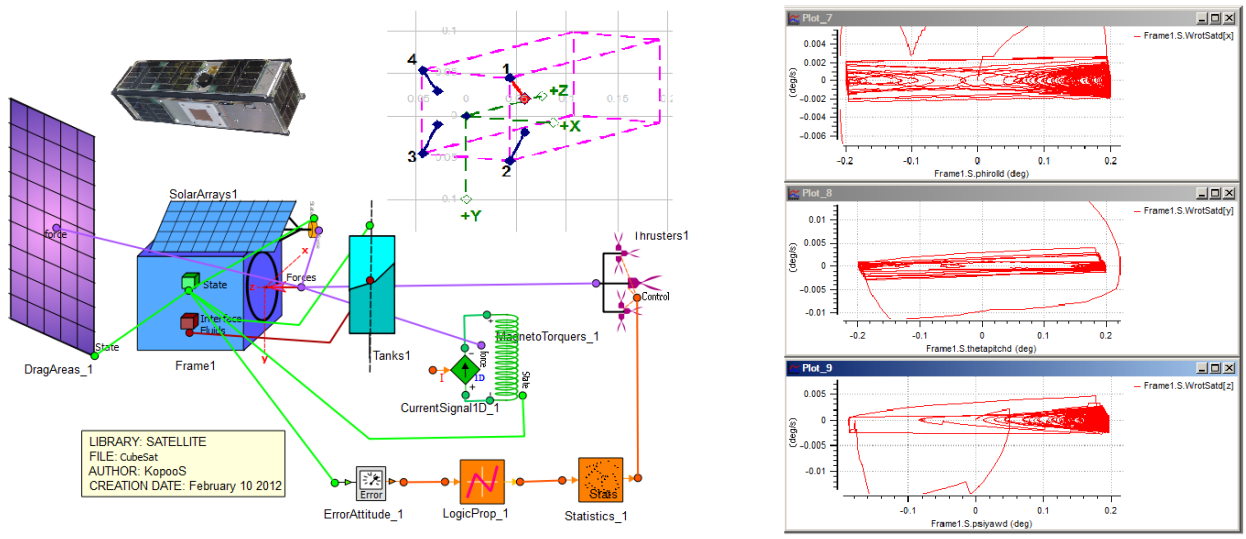

Figure 9. Simulation model for active "All EP" ACS and outputs of the attitude control $\pm 0.2°$ in phase diagram.

VI. Conclusion

A novel liquid-fed PPT concept has been proposed, based on a non-volatile propellant. While the propellant's properties are in many aspects reminiscent of PTFE, the possibility to feed it through a capilary was leveraged to separate the ablation phase from the ionization/acceleration phase, using flashover discharge ablation over the free surface of the propellant. This design is expected to significantly reduce late-time ablation due to the small area of the capillary subjected to thermal ablation from the main discharge.

As with other liquid propellant thrusters but unlike solid propellant PPTs, this propulsion system also benefits from the possibility to balance the propellant consumption between several thrusters using a common tank.

The first proof-of-concept prototypes of the thruster, electronics, tank, injector and thrust balance have been manufactured and have already been subjected to a number of functional tests. Testing in vacuum is nearly complete for the propellant and injector assembly, and thruster tests in vacuum are expected to follow soon. In parallel with these tests, several mission scenarios have been investigated which shall be used as input for the second set of prototypes.

Ackowledgments

The research leading to these results has received funding from the European Community's Seventh Framework Programme (FP7/2007-2013) under grant agreement n°283279 for the L-µPPT project. IPPLM has also received financial support from the Polish fund for science in years 2012-2014 for the execution of a partially funded international project.

References

[1]Mueller, J., "Thruster Options for Microspacecraft," *Proc. 33rd AIAA Joint Propulsion Conference*, No. 1997-3058, American Institute of Aeronautics and Astronautics, Washington, D.C., Seattle, WA, 1997.

[2]Guarducci, F., Coletti, M., and Gabriel, S. B., "Design and Testing of a Micro Pulsed Plasma Thruster for Cubesat Application," *Proc. 32nd International Electric Propulsion Conference*, No. 2011-239, The Electric Rocket Propulsion Society, Worthington, OH, Wiesbaden (Germany), 2011.

[3]Shaw, P. V., Lappas, V. J., and Underwood, C. I., "Design, Development and Evaluation of an 8 µPPT Propulsion Module for a 3U CubeSat Application," *Proc. 32nd International Electric Propulsion Conference*, No. 2011-115, The Electric Rocket Propulsion Society, Worthington, OH, Wiesbaden (Germany), 2011.

[4]Ziemer, J. K. and Petr, R. A., "Performance of Gas Fed Pulsed Plasma Thrusters Using Water Vapor Propellant," *Proc. 38th AIAA Joint Propulsion Conference*, No. 2002-4273, American Institute of Aeronautics and Astronautics, Washington, D.C., Indianapolis, 2002.

[5]Scharlemann, C. A., *Investigation of Thrust Mechanism in a Water Fed Pulsed Plasma Thruster*, Ph.D. thesis, Ohio

State University, 2003.

[6]Koizumi, H., Kakami, A., Furuta, Y., Komurasaki, K., and Arakawa, Y., "Liquid Propellant Pulsed Plasma Thruster," *Proc. 28th International Electric Propulsion Conference*, No. 2003-87, The Electric Rocket Propulsion Society, Worthington, OH, Toulouse (France), 2003.

[7]Kakami, A., Koizumi, H., Komurasaki, K., and Arakawa, Y., "Design and Performance of Liquid Propellant Pulsed Plasma Thruster," *Vacuum*, Vol. 73, 2004, pp. 419.

[8]Koizumi, H., Komurasaki, K., and Arakawa, Y., "Development of Thrust Stand for low Impulse Measurement from Microthrusters," *Rev. Sci. Instrum.*, Vol. 75, 2004, pp. 3185.

[9]Koizumi, H., Kawazoe, Y., Komurasaki, K., and Arakawa, Y., "Performance Improvement of a Liquid Propellant Pulsed Plasma Thruster," *Proc. 29th International Electric Propulsion Conference*, No. 2005-69, The Electric Rocket Propulsion Society, Worthington, OH, Princeton, NJ, 2005.

[10]Zhu, P., Hou, L. Y., and Zhang, W. Y., "The Effect of Easily Ionized Elements Na and K on the Performance of Pulsed Plasma Thruster using Water Propellant," *Sci Tech China Sci*, Vol. 53, 2010, pp. 2878.

[11]Böhrk, H., Lau, M., Herdrich, G., Hald, H., and Röser, H.-P., "A Porous Flow Control Element for Pulsed Plasma Thrusters," *CEAS Space J.*, 2011, pp. 1.

[12]Shaw, P. V. and Lappas, V. J., "Modeling of a Pulsed Plasma Thruster; Simple Design, Complex Matter," *Proc. Space Propulsion 2010*, San Sebastian (Spain), 2010.

[13]Colleti, M., Guarducci, F., and Gabriel, S. B., "A micro PPT for Cubesat Application: Design and Preliminary Experimental Results," *Acta Astronautica*, Vol. 66, 2010, pp. 1534.

[14]Burton, R. L. and Turchi, P. J., "Pulsed Plasma Thruster," *J. Propul. Power*, Vol. 14, 1998, pp. 716.

[15]"Busek's Micro Pulsed Plasma Thrusters (µPPTs)," http://www.busek.com.

[16]Rayburn, C., Campbell, M., Hoskins, W. A., and Cassady, J. R., "Development of a Micro Pulsed Plasma Thruster for the Dawgstar Nanosatellite," *Proc. 36th AIAA Joint Propulsion Conference*, No. 2000-3256, American Institute of Aeronautics and Astronautics, Washington, D.C., Huntsville, AL, 2000.

[17]Spanjers, G. G., Bromaghim, D. R., Lake, J., Dulligan, M., White, D., Schilling, J. H., Bushman, S., Antonsen, E. L., Burton, R. L., Keidar, M., and Boyd, I. D., "AFRL MicroPPT Development for Small Spacecraft Propulsion," *Proc. 38th AIAA Joint Propulsion Conference*, No. 2002-3974, American Institute of Aeronautics and Astronautics, Washington, D.C., Indianapolis, 2002.

[18]Wie, B., Murphy, D., Paluszek, M., and Thomas, S., "Robust Attitude Control Systems Design for Solar Sails, Part 2: MicroPPT-based Secondary ACS," *Proc. 40th AIAA Joint Propulsion Conference*, No. 2004-5011, American Institute of Aeronautics and Astronautics, Washington, D.C., Fort Lauderdale, FL, 2004.

[19]http://www.bartels-mikrotechnik.de.

[20]http://www.curiejet.com.

[21]http://www.takasago-fluidics.com.

[22]Kiesel, F. and Degen, R., "Ultra Compact and Light-Weight Micro-Actuators suitable for Space Applications," *14th European Space Mechanisms & Tribology Symposium – ESMATS 2011*, Constance (Germany), 2011.

[23]Haag, T. W., "Thrust Stand for Pulsed Plasma Thrusters," *Rev. Sci. Instrum.*, Vol. 68, 1997, pp. 2060.

[24]Cubbin, E. A., Ziemer, J. K., Choueiri, E. Y., and Jahn, R. G., "Pulsed Thrust Measurements using Laser Interferometry," *Rev. Sci. Instrum.*, Vol. 68, 1997, pp. 2339.

[25]Gamero-Castaño, M., "A Torsional Balance for the Characterization of MicroNewton Thrusters," *Rev. Sci. Instrum.*, Vol. 74, 2003, pp. 4509.

[26]D'Souza, B. C. and Ketsdever, A. D., "Investigation of Time-Dependent Forces on a Nano-Newton-Second Impulse Balance," *Rev. Sci. Instrum.*, Vol. 76, 2005, pp. 015105.

[27]Ketsdever, A. D., D'Souza, B. C., and Lee, R. H., "Thrust Stand Micromass Balance for the Direct Measurement of Specific Impulse," *J. Propul. Power*, Vol. 24, 2008, pp. 1376.

[28]Lilly, T., Pancotti, A., Ketsdever, A., Young, M., and Duncan, J., "Development of a Specific Impulse Balance for a Pulsed Capillary Discharge," *Proc. 44th AIAA Joint Propulsion Conference*, No. 2008-4740, American Institute of Aeronautics and Astronautics, Washington, D.C., Hartford, CT, 2008.

[29]Erichsen, P., "Performance Evaluation of Spacecraft Propulsion Systems in Relation to Mission Impulse Requirements," *Proc. 2nd European Spacecraft Propulsion Conference, ESA SP-398*, Noordwijk (Netherlands), 1997.

[30]Mauthe, S., Pranajaya, F., and Zee, R. E., "The Design and Test of a Compact Propulsion System for CanX Nanosatellite Formation Flying," *19th Annual AIAA/USU Conference on Small Satellites*, No. VI-5, Logan, UT, 2005.

[31]Selva, D. and Krejci, D., "A Survey and Assessment of the Capabilities of CubeSats for Earth Observation," *Acta Astronautica*, Vol. 74, 2012, pp. 50.

[32]Cote, K., Gabriel, J., Patel, B., Ridley, N., Taillefer, Z., and Tetreault, S., *Mechanical, Power, and Propulsion Subsystem Design for a CubeSat*, Bachelor's thesis, Worcester Polytechnic Institute, 2011.

[33]Hinkley, D. and Hardy, B., "Picosatellites and Nanosatellites at the Aerospace Corporation," *In-Space Non-Destructive Inspection Technology Workshop*, Houston, TX, 2012.

[34]Andersson, B. et al., "Attitude and Orbit Control Systems for GEO Bird only Based on Electric Propulsion," *Proc. Space Propulsion 2012*, Bordeaux (France), 2012.

[35]Stoltz, S., Courtois, K., Raschke, C., and Baumann, F., "The World's Smallest Reaction Wheel – The Development, Fields of Operation and Flight Results of the RW 1," *Advances in the Astronautical Sciences*, Vol. 137, 2010, pp. 821.

[36]"ESPSS: European Space Propulsion System Simulation library for EcosimPro tool." .